



## Thermal Hydraulic Performance Asymmetric Aero Foil Fin in Printed Circuit Heat Exchanger

Donny Nurmayady<sup>1\*</sup>, Mita Konstantin<sup>2</sup>, Khairul Handono<sup>3</sup>, Arief Tris Yulianto<sup>4</sup>, Erwin Nashrullah<sup>5</sup>, Nurlaila<sup>1</sup>, Devita Nitiamijaya<sup>1</sup>, Jentik Meikayani<sup>1</sup>, Muhammad Zulham Kentji<sup>6</sup>

<sup>1</sup> Research Center for Nuclear Reactor Technology, National Research and Innovation Agency of Indonesia, Kawasan Sains dan Teknologi, BJ Habibie, Office Building, 720, Tangerang Selatan, Banten, Indonesia 15310

<sup>2</sup> Binus University, The Joseph Wibowo Center (JWC) Jl. Hang Lekir 1 no. 6, Senayan Jakarta 10270, Indonesia

<sup>3</sup> Research Center for Nuclear Beam Analysis Technology, National Research and Innovation Agency of Indonesia, Kawasan Sains dan Teknologi, BJ Habibie, Office Building, 720, Tangerang Selatan, Banten, Indonesia 15310

<sup>4</sup> Directorate for Policy Evaluation of Research, Technology, and Innovation, National Research and Innovation Agency of Indonesia, Gedung BJ Habibie, Jl. M.H. Thamrin Nomor 8 Jakarta Pusat – Indonesia 10340

<sup>5</sup> Research Center for Energy Conversion and Conservation, National Research and Innovation Agency of Indonesia, Kawasan Sains dan Teknologi, BJ Habibie, Office Building, 720, Tangerang Selatan, Banten, Indonesia 15310

<sup>6</sup> Faculty of Electricity and Renewable Energy, Institute Technology of PLN (IT-PLN), Menara PLN, Jl. Lkr. Luar Barat Lantai 2, RT.1/RW.1, Duri Kosambi, Kecamatan Cengkareng, Kota Jakarta Barat, Daerah Khusus Ibukota Jakarta 11750

### ARTICLE INFO

#### Article history:

Received: November 6, 2025

Received in revised form: Nov. 21, 2025

Accepted: December 10, 2025

#### Keywords:

printed circuit heat exchanger

aerofoil fin

carbondioxide

thermal hydraulic

pressure drop

heat transfer rate

### ABSTRACT

Aligning with the development of an advanced reactor in SMR design, a compact heat exchanger was considered important. Printed Circuit Heat Exchanger (PCHE) is a compact heat exchanger with the smallest dimensions among industrial heat exchangers. Many innovative designs have been published regarding thermal-hydraulic performance as well as architecture or structure in PCHE. This paper shows a comparison of airfoil fin shapes. The purpose of this study is to compare thermal hydraulic performance between symmetric and asymmetric airfoil fins in Printed Circuit Heat Exchanger (PCHE) using three different gases, i.e., Nitrogen, Carbon dioxide, and Hydrogen. One row of 3-D airfoils has been analyzed with the Nusselt number, pressure drop, and heat transfer coefficient compared. A simulation

has been done on the finite element method using COMSOL software to demonstrate the structures, the heat transfer profile, as well as thermal-hydraulic numbers. The asymmetrical aerofoil has about 23.38% higher heat transfer rate and 19.67% lower pressure drop compared to the Air Foil Fin (symmetrical aerofoil). It is concluded that an asymmetric aerofoil using carbon dioxide would provide the smallest physical dimension, followed by the lowest pressure drop.

© 2025 Tri Dasa Mega. All rights reserved.

## 1. INTRODUCTION\*

The Research Center for Nuclear Reactor Technology of Indonesia organizes a conceptual design study of a High Temperature Gas-cooled

Reactor (HTGR) with a thermal power of 30 MW<sub>th</sub>, called PeLUIt-40. This innovative reactor is designed not only to generate electricity but also to produce hydrogen as part of a cogeneration system. The PeLUIt-40 represents a notable advancement in Indonesia's commitment to both clean energy

\*Corresponding author. Tel./Fax.: + 62 812-8289-0793

E-mail: [donn004@brin.go.id](mailto:donn004@brin.go.id)

DOI: 10.55981.tdm.2025.13639

initiatives and technological progress [1]. High Temperature Gas-cooled Reactor (HTGR) is an inherent safety reactor and able to provide high temperature steam and/or fluids (between 650°C and 950°C) at the reactor outlet. This technology is comprised of the three major components: reactor, heat exchanger, and power conversion system. In the recent report [2], the development of HTGR tends to couple power generation and hydrogen production. The steam turbine is still the major power conversion plant to be used.

A heat exchanger is the main component in transferring energy from the heat source to the secondary system. The effectiveness and heat transfer rate will have a significant impact on the cycle efficiency. A good performance on the heat exchanger is also determined by its ability to preserve a high heat transfer rate. Printed Circuit Heat Exchanger (PCHE) or Microchannel Heat Exchanger is the most reliable type of heat exchanger to gain high performance [3]. Zohuri [4] suggested that Printed Circuit Heat Exchanger (PCHE) usage would be a prominent research topic in HTGR; furthermore, it is a requirement for hydrogen production. Helium is commonly used in HTGR, particularly in the primary system (reactor side). Due to inertness, limited design power conversion [3] as well as a lack of sensitivity to the change in the Helium pressure for the secondary system [5], suitable working fluid in the secondary system of PCHE should be investigated.

Various outstanding types of PCHE flow channels have been developed so far and have a considerable results. Semi semi-circular channel was used by S.J. Yoon, et. al [6] to investigate Nusselt number and friction factor correlations for laminar flow. Zhang YD., et. al [7] analysed local heat transfer convection while Ren Z, et. al [8] analysed local heat transfer during the cooling stage, and Zhang H., et. al [9] analysed buoyancy effects on coupled heat transfer in the SCO<sub>2</sub> cycle.

Regarding flow path, thermal-hydraulic was investigated in straight channels by A.M. Aneesh et. al [10] in 3D view, J.W. Seo, et. al [11] to determine heat transfer and pressure drop, and Chu WX., et. al [12] for their novel hyperbolic inlet header. Wavy channels, zigzag channels, or sinusoidal channels were applied to determine thermal hydraulic performance by Wang J., et. al [13] for sinusoidal channeled, Chen MH., et. al [14] for zigzag flow channels and Y.J. Baik, et. al [15] for the effect of waviness.

Besides various channel configurations research in PCHE, there are some studies applying obstacles to the flow to generate vortex heat. These obstacles are embedded in the channel. Various

shapes and dimensions have been investigated, such as fins, S-shaped, dimples, etc. A.M. Aneesh, et. al [10] applied dimples in the straight channel of PCHE to analyse flow performance. A novel arc-shaped structure was analysed by S.M. Lee et al [16] applying multi-objective optimisation. Thermal-hydraulic analysis was investigated by applying an S-shaped or sinusoidal fin-based [17] as well as a discontinuous fin [18]. Straight channel, zigzag channel, S-shape, and aerofoil fin have been compared by Kim In Hun, et. al [19] to determine performance as well as cost assessment. Research on applying an aerofoil fin (AFF) in PCHE has been increasing in the last decade [20], in terms of optimisation [21], hydraulic and thermal performance [22] as well as placement configuration [23]. The shape of the NACA series, which is common in aeronautical engineering, inspired researchers to apply it in PCHE [24].

According to the studies above, this paper would contribute to proposing a new fin structure as a novel contribution for PCHE research and development, called asymmetric AFF. It described a comparison thermal-hydraulic analysis between symmetric AFF and novel asymmetric AFF in three different gases (Nitrogen, Hydrogen, and Carbon dioxide). The purpose of this research is to determine the heat transfer rate as well as the pressure drop among three different gases. Hence, the decision to select the best thermal hydraulic performance PCHE as well as the gas applied will be made. Some challenges, such as a high effectiveness constant value of heat exchanger selection and optimisation performance of the working fluid, needed to be addressed. An interaction between the heat exchanger and working fluid performance was simulated in COMSOL Multiphysics Software. COMSOL is a package of software for analysis, solver, and simulation of coupled phenomena and multiphysics, as well as various physical and engineering applications based on the finite element method. This asymmetric AFF shape gains a similar heat transfer rate to symmetric AFF and a better flow reduction as the tail is thinner and pointed up. This study may contribute to the PeLUit-40 project since the reactor is an advanced nuclear power plant. PeLUit-40 is an HTGR type and an advanced reactor that requires a compact heat exchanger [4].

## 2. THEORY

Thermal-hydraulic parameter performance will be measured, such as Nusselt number, Pressure drop, and heat transfer coefficient. This work will compare symmetrical and non-symmetrical aerofoils using three different gases (Nitrogen, Hydrogen, and Carbon dioxide). The main concern of this research is to

investigate the best performance of those gases in PCHE shapes. Another objective of this study is to find a suitable working fluid for PCHE in an HTGR power station. COMSOL software was used to calculate the heat transfer coefficient as well as the pressure drop of the channel using the finite element method.

All calculation methods being considered were retrieved from Cengel (2008) [25]. A List of nomenclature is attached in the appendix. Overall heat transfer coefficients were determined by using

$$U_A = \frac{dQ}{dA (T_{wall} - \frac{T_{out} - T_{in}}{2})} \quad (1)$$

Nusselt number (Nu) shows heat transfer across the boundary, either convective or conductive. It can also indicate the type of flow, turbulent or laminar. A larger Nusselt number indicates a higher convection coefficient, with turbulent flow typically in the 100–1000 range.

$$Nu = \frac{U_A \cdot D_h}{k} \quad (2)$$

Where,  $U_A$  is the overall heat transfer coefficient, and  $k$  is the thermal conductivity.  $D_h$  is the hydrodynamic diameter.

$$D_h = \frac{4A}{P} \quad (3)$$

Hydrodynamic diameter is the length that consists of four cross-sectional areas ( $A$ ) and wetted perimeter ( $P$ ) of the fluid flow. COMSOL can also calculate the pressure drop, which refers to

$$\Delta P = \frac{64}{Re_D} \frac{\rho \cdot v^2 \cdot L}{D_h} \quad (4)$$

Where,  $Re_D$  is the Reynolds number,  $\rho$  is fluid density,  $D_h$  is the hydrodynamic diameter,  $v$  is the velocity of the fluid, and  $L$  is the length of the channel. The Reynolds number indicates the type of flow, laminar or turbulent. Thus, the viscosity,  $\mu$ , of the fluid affects the value of  $Re$ .

$$Re_D = \frac{\rho \cdot v \cdot D_h}{\mu} \quad (5)$$

This subsection explains how an airfoil fin can increase the heat transfer rate. Fins affect the flow and heat transfer of a heat exchanger mainly in two ways, i.e., enlarging the heat transfer area and causing disturbance. Conductive and convective heat transfer between the fluid and the boundary channel (including the fin) will affect the size of heat transfer. When the flow passes through the fin, a little chaotic flow may generate an eddy or a little swirl at the tail of the airfoil,

hence will contribute to the thermal hydraulic performance. However, Fin also generates a pressure drop as a result of the disturbance.

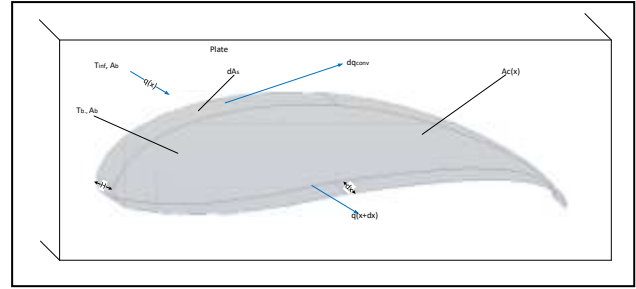


Figure 1. Aerofoil fin analysis

Figure 1 shows the Aerofoil fin structure, in which:

- $T_b, A_b$  is the area temperature and area of the fin from its base (the plate)
- $H_b$  is the Height of the fin (in the  $x$ -location)
- $T_\infty$  is the ambient temperature of the environment (assumed constant in all surfaces)
- $h$  is the convection coefficient between the fin and the ambient environment (assumed constant)
- $A_c(x)$  for the cross-sectional area of the fin at the location  $x$
- $dA_s$  is the surface area around the perimeter of the differential element, at location  $x$
- $dq_{conv}$  is the heat flow rate from the surface area around the perimeter of the differential element, by convection, at the location  $x$
- $q(x)$  is the heat flow rate conduction into the element at the location  $x$
- $q(x + dx)$  is the heat flow rate conduction out of the element at the location of  $x + dx$

The energy that exists the element was assumed to be equal to the energy that enters the element in a steady-state heat flow operating condition. Hence, the energy balance would be

$$q(x) = q(x + dx) = dq_{conv} \quad (6)$$

By Newton's law

$$dq_{conv} = h \cdot dA_s (T(x) - T_\infty) \quad (7)$$

For  $dx \rightarrow 0$ , the formulae become

$$\frac{dq(x)}{dx} = -h \cdot dA_s (T(x) - T_\infty) \quad (8)$$

$h$  is the heat transfer coefficient. From Fourier's law, the equation becomes as follows, with  $k$  as the thermal conductivity of the aerofoil material.

$$q(x) = -k \cdot A_c(x) \frac{dT(x)}{dx} \quad (9)$$

Substitution and simplification of the above equations result in the final general differential equation for one-dimensional steady state heat transfer from an extended surface (given below). Hence, the temperature distribution  $T(x)$  can be estimated based on the boundary conditions being selected,

$$\frac{d^2 T(x)}{dx^2} + \left( \frac{1}{A_c(x)} \frac{dA_c(x)}{dx} \right) \frac{dT(x)}{dx} - \left( \frac{1}{A_c(x)k} \frac{h dA_s(x)}{dx} \right) (T(x) - T_\infty) = 0 \quad (10)$$

To get an idea of how the aerofoil can increase heat transfer, the aerofoil was assumed to have a constant cross-sectional area, where  $A_c(x) = A_c$ . Then  $\frac{dA_c(x)}{dx} = 0$  in the above equation, and  $\frac{dA_s(x)}{dx} = P$ , where  $P$  is the perimeter (with  $A_s(x) = Px$ ), the above equation then becomes,

$$\frac{d^2 T(x)}{dx^2} - \left( \frac{h \cdot P}{kA_c} \right) (T(x) - T_\infty) = 0 \quad (11)$$

The two boundary conditions were implemented in the  $x$  direction due to the second-order differential equations. The first boundary condition as  $T(0) = T_b$ , and for the second boundary condition, as negligible heat transfer at the tip, at  $x = H$ , hence,  $q(H) = 0$ . These assumptions were set because it's relative to its width, since the longer the fin is, the closer its tip temperature is to the ambient temperature  $T_\infty$ . Thus, the temperature gradient  $T(x)$  at the tip approaches zero. By Fourier's law, meaning that the heat flow out of the tip approaches zero.

Refer to equation (4) for the temperature distribution  $T(x)$ , the heat transfer rate  $q_f$  at the base of the airfoil (at  $x = 0$ ) was assumed. Hence, solving for  $T(x)$  and substituting into the above equation,

$$q_b(0) = h \cdot A_c \cdot (T_b - T_\infty) \quad (12)$$

The aerofoil may increase heat transfer by calculating the following ratio

$$\frac{q_f(0)}{q_b(0)} = \sqrt{\frac{P^2}{(A_c)^2}} \cdot H \quad (13)$$

### 3. METHODOLOGY

There are a large number of special geometries in an industrial heat exchanger. Suitable geometries were compared to determine the heat transfer coefficients or dimensionless heat transfer parameters (i.e., Nusselt number, Stanton number, etc.) for the selected surfaces. Enhanced surfaces provide a greater heat

transfer coefficient; however, they may increase fluid flow friction and pressure drop. A printed circuit heat exchanger (PCHE) produced by Heatric [26] is chosen. This PCHE has been investigated to support the Feher cycle with acceptable dimensions to perform in high pressures and high temperatures. Recent PCHEs have a maximum dimension of 600 mm width, 600 mm height, and 1500 mm length. Several modules can be attached side by side and create larger and more complex heat exchanger assemblies. Figure 2 depicts a real printed circuit heat exchanger.



Figure 2. Printed Circuit Heat Exchanger (Heatric) [26]

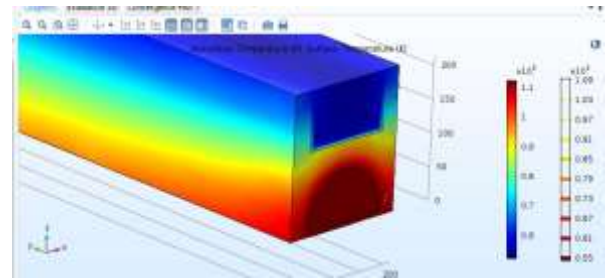


Figure 3. PCHE Heat transfer profile in COMSOL

Figure 3 shows the frontal area of one channel (primary) for Helium at the bottom and another (secondary) channel for other gases (Nitrogen, Hydrogen, or Carbon dioxide). The inlet temperature of those gases is set at 300 K (26.85 °C), while in the hot channel (Helium) is constant at 1123 K (849.85 °C). Several attempts have been made to investigate output temperature in the cold channel. The results remain similar among those three gases, about 950 K (676.85 °C). It is consuming time and requiring a powerful computer to simulate the entire heat exchanger geometry. Therefore, in this simulation, hot channel parameters are replaced by the initial condition of 1123 K (849.85 °C). Thus, only the cold channel is simulated to compare thermal-hydraulic performance amongst gases and the aerofoil fin. The inlet velocity was set to 0.5, 1.0, 2.5, and 5.0 m/s. Actual PCHE might use a zig-zag channel profile; however, in this work, only straight channels are considered.

Aerofoils are determined by three-dimensional geometry: length ( $L$ ) of the aerofoil is 4 mm, width ( $W$ ) is 1 mm, and height ( $H$ ) is 0.5 mm. Each space between aerofoils is 1 mm, as can be seen in Figure 4. Figure 5 shows aerofoils in a metal plate, and only one

row will be investigated. Each row has a geometry of the channel of  $1 \text{ mm} \times 2 \text{ mm} \times 30 \text{ mm}$  with 10 aerofoils. The similar assumptions using Alloy 800H for the material of the plate were applied, with a density of  $7800 \text{ kg/m}^3$ , specific heat of  $420 \text{ kJ/kg}$ , and thermal conductivity of  $15 \text{ W/m-K}$ .

The commercial software COMSOL with the self-library real gas property tables is used to study this simulation research. The boundary layers were set, such as near the top and bottom walls and fin surfaces, and the thickness of the first layer is  $0.001 \text{ mm}$ . After carefully checking for the degree of freedom meshing grid for the numerical solution, the grid system was 1004780 cells, and it took about 35 minutes for each simulation.

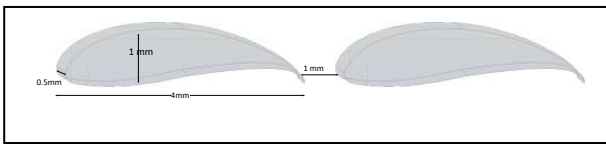


Figure 4. Asymmetrical aerofoil



Figure 5. Symmetrical and asymmetrical aerofoil

Figure 3 is a symmetrical aerofoil or Aero Foil Fin (AFF), while Figure 4 is a proposed new non-symmetrical aerofoil. Due to long computation, only one row of the aerofoil will be investigated.

COMSOL calculates the aforementioned PCHE heat transfer profile seen in Figure 2, which consists of the heat transfer rate and the pressure drop. Hence, the Nusselt number and Reynolds number were determined to know the characteristics of heat transfer as well as the fluid flow pattern. The brief dimension of PCHE was analyzed by comparing thermal hydraulic parameters (pressure drop and heat transfer rate) per dimension parameter.

#### 4. RESULTS AND DISCUSSION

Previous studies on research aimed to have a lower pressure drop by utilizing other shapes. The symmetric and asymmetric airfoils were compared in this work, comparing flow characteristics by utilizing various gases (Nitrogen, Hydrogen, and Carbon dioxide).

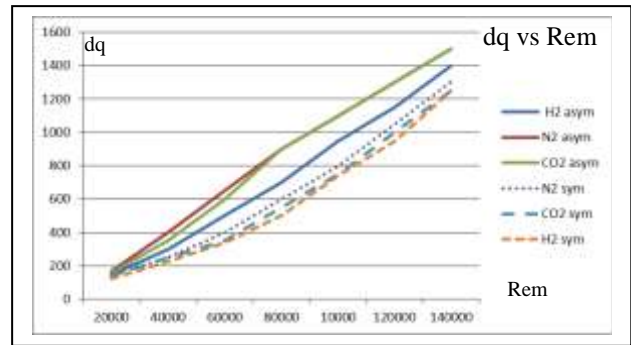


Figure 6. Ratio of total heat transfer and fluid flow patterns.

Nusselt number,  $Nu$ , represents the ratio of total heat transfer, which is the ability to transfer heat in the channel, while  $Re$  represents the speed and pattern of flow in a channel. As seen in Figure 6, all values of the asymmetric aerofoil fin are higher than those of the symmetric aerofoil fin due to the thickness of the aerofoil fin. The thickness affects the hydraulic diameter. Regarding working gases, Nitrogen and Carbon dioxide have a high Nusselt number, which means that using these gases as working fluid requires a high mass flow rate as the gas has poor thermal conductivity.

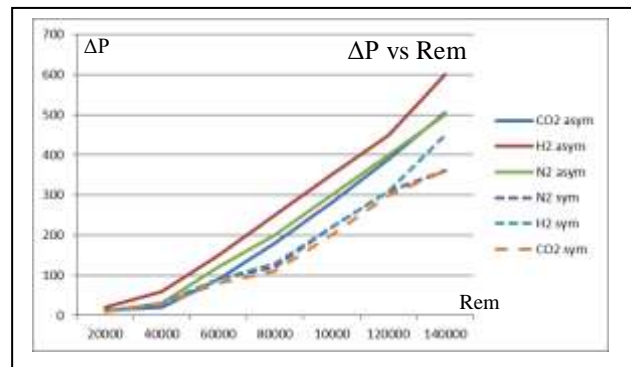
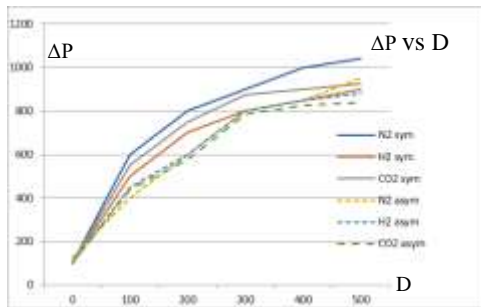


Figure 7. Pressure drop and fluid flow pattern

Figure 7 shows the pressure drop characteristic over Reynolds number. The pressure drop over the length of the channel was determined to analyze the lowest dimension of the overflow pattern. Using an asymmetric aerofoil fin, the pressure drop was higher than symmetric aerofoil fin due to the difference in thickness in the asymmetric aerofoil fin. Hence, Reynolds numbers were high due to generation of vortex generation in the point-down tail of the asymmetric aerofoil fin. Regarding using Hydrogen as a working gas, this gas generated a higher pressure drop due to its lowest viscosity, although the gas has the highest thermal conductivity. However, it might be possible to use Hydrogen in a laminar flow pattern. Referring to equation (4), the pressure drop is affected by flow.



**Figure 8.** Pressure drop and dimension of the channel heat exchanger

Figure 8 shows the pressure drop of the channel to show thermal hydraulic performance regarding the dimensions of the channel, related to the smallest dimension of the channel needed. The asymmetric aerofoil using carbon dioxide was the lowest, showing that the heat exchanger dimension as well as the pressure drop were the lowest. Thus, an asymmetric aerofoil using carbon dioxide would be the smallest physical dimension and the lowest pressure drop.

Overall, the asymmetric aerofoil has a better heat transfer rate and lower pressure drop (23.73% and 19.68%) due to the different shape of the aerofoil. An asymmetric aerofoil has a smaller hydraulic diameter and a tail pointed down, inducing a little swirl flow. It was observed that a narrower aerofoil would make a larger heat transfer rate, followed by an increase in flow velocity in the aerofoil

## 5. CONCLUSION

A study of thermal hydraulic performance between an asymmetric aerofoil fin and a symmetric aerofoil fin shows that the Nusselt number and pressure drop per unit length increase as the inlet Reynolds number increases in all results. An asymmetric aerofoil has a better heat transfer rate and lower pressure drop (23.73 % and 19.68 %) due to the different shape of the aerofoil. An asymmetric aerofoil using carbon dioxide would have the smallest physical dimension and the lowest pressure drop.

## ACKNOWLEDGMENT

Most of this work was financially supported by the Riset-PRO Project from the Ministry of Research and Technology of Indonesia in 2016-2021. The author also appreciates the Head of the Research Center for Nuclear Reactor Technology and BRIN of Indonesia for his support in finishing this paper.

## AUTHOR CONTRIBUTION

**Donny Nurmayady:** Writing – review, Original draft, Conceptualization, Methodology, Investigation, Funding acquisition, Data curation, Formal analyses. **Mita Konstantin:** Writing–systematic literature review, Original draft, Methodology. **Khairul Handono:** Conceptualization, Writing review & editing, Methodology. **Arief Tris Yulianto:** Writing – review, Investigation, Funding Acquisition, Data curation. **Erwin Nashrullah:** Writing–review, Validation, Conceptualization, Supervision. **Nurlaila:** Format analysis, Writing – review, Editing, Data curation, Methodology, Investigation. **Devita Nitiamijaya:** Editing, Format analysis, Investigation, Writing–editing, Visualization, Project Administration. **Jentik Meikayani:** Investigation, Visualization, Writing – editing. **Muhammad Zulham Kentji:** Conceptualization, Writing review & editing, Methodology.

## REFERENCES

1. Antaranews.com *BRIN Outlines Development plans for Nuclear Power Plant in Indonesia*, Available from: <https://en.antaranews.com/news/316473/brin-outlines-development-plans-for-nuclear-power-plant-in-indonesia>.
2. IAEA Advances in Small Modular Reactor Technology Developments. A Suppl. to IAEA Adv. React. Inf. Syst. 2020 Ed. 2020.:354.
3. Olumide Olumayegun, Meihong Wang G.K. Thermodynamic Analysis and Preliminary Design of Closed Brayton Cycle using Nitrogen as Working Fluid and Coupled to Small Modular Sodium-cooled Fast Reactor (SM-SFR). *Appl. Energy*. 2017. **191**:436–53.
4. Zohuri B. Nuclear Energy for Hydrogen Generation through Intermediate Heat Exchangers: A Renewable Source of Energy. 2016.
5. Chai L., Tassou S.A. A Review of Printed Circuit Heat Exchangers for Helium and Supercritical CO<sub>2</sub> Brayton cycles. 2020.
6. Yoon S.J., O'Brien J., Chen M., Sabharwall P., Sun X. Development and Validation of Nusselt Number and Friction Factor Correlations for Laminar Flow in a Semi-circular Zigzag Channel of a Printed Circuit Heat Exchanger. *Appl. Therm. Eng.* 2017. **123**:1327–44.
7. Zhang Y., Peng M., Xia G., Cong T. Numerical Investigation on Local Heat Transfer Characteristics of S-CO<sub>2</sub> in Horizontal Semicircular Microtube. *Appl. Therm. Eng.* 2019. **154**(July 2018):380–92.

8. Ren Z., Zhao C.R., Jiang P.X., Bo H.L. Investigation on Local Convection Heat Transfer of Supercritical CO<sub>2</sub> during Cooling in Horizontal Semicircular Channels of Printed Circuit Heat Exchanger. *Appl. Therm. Eng.* 2019. **157**(April):113697.
9. Zhang H., Guo J., Huai X., Cui X., Cheng K. Buoyancy Effects on Coupled Heat Transfer of Supercritical Pressure CO<sub>2</sub> in Horizontal Semicircular Channels. *Int. J. Heat Mass Transf.* 2019. **134**:437–49.
10. Aneesh A.M., Sharma A., Srivastava A., Vyas K.N., Chaudhuri P. Thermal-hydraulic Characteristics and Performance of 3D Straight Channel-based Printed Circuit Heat Exchanger. *Appl. Therm. Eng.* 2016. **98**:474–82.
11. Seo J.W., Kim Y.H., Kim D., Choi Y.D., Lee K.J. Heat Transfer and Pressure Drop Characteristics in Straight Microchannel of Printed Circuit Heat Exchangers. *Entropy*. 2015. **17**(5):3438–57.
12. Chu W. xiao, Bennett K., Cheng J., Chen Y. Tung, Wang Q. Wang Numerical Study on a Novel Hyperbolic Inlet Header in Straight-Channel Printed Circuit Heat Exchanger. *Appl. Therm. Eng.* 2019. **146**(April 2018):805–14.
13. Wang J., Sun Y., Lu M., Wang J., Yan X. Study on the Thermal-hydraulic Performance of Different Channels in Printed Circuit Heat Exchanger. *Energy Procedia*, 158 (6) 2019. 5679-5684.
14. Chen M., Sun X., Christensen R.N. Thermal-hydraulic Performance of Printed Circuit Heat Exchangers with Zigzag Flow Channels. *Int. J. Heat Mass Transf.* 2019. **130**:356–67.
15. Baik Y.J., Jeon S., Kim B., Jeon D., Byon C. Heat Transfer Performance of Wavy-channeled PCHEs and the Effects of Waviness Factors. *Int. J. Heat Mass Transf.* 2017. **114**:809–15.
16. Lee S.M., Kim K.Y. Multi-objective Optimization of Arc-shaped Ribs in the Channels of a Printed Circuit Heat Exchanger. *Int. J. Therm. Sci.* 2015. **94**:1–8.
17. Saeed M., Kim M.H. Thermal-hydraulic Analysis of Sinusoidal Fin-based Printed Circuit Heat Exchangers for Supercritical CO<sub>2</sub> Brayton cycle. *Energy Convers. Manag.* 2019. **193**(April):124–39.
18. Pidaparti S.R., Ranjan D., Anderson M. Thermal-hydraulic Performance of Discontinuous fin Heat Exchanger Geometries using Supercritical CO<sub>2</sub> as the Working Fluid. 6th Int. Symp. - Supercrit. CO<sub>2</sub> Power Cycles. 2018.
19. Kim I.H., Zhang X., Christensen R., Sun X. Design Study and Cost Assessment of Straight, Zigzag, S-shape, and OSF PCHEs for a FLiNaK–SCO<sub>2</sub> Secondary Heat Exchanger in FHRs. *Ann. Nucl. Energy*. 2016. **94**:129–37.
20. Liu G., Huang Y., Wang J., Liu R. A Review on the Thermal-hydraulic Performance and Optimization of Printed Circuit Heat Exchangers for Supercritical CO<sub>2</sub> in Advanced Nuclear Power Systems. *Renew. Sustain. Energy Rev.* 2020. **133**(August):110290.
21. Kwon J.G., Kim T.H., Park H.S., Cha J.E., Kim M.H. Optimization of Airfoil-type PCHE for the Recuperator of Small Scale Brayton Cycle by Cost-based Objective Function. *Nucl. Eng. Des.* 2016. **298**:192–200.
22. Chu W. Xiao, Li X. Hui, Ma T., Chen Y. Tung, Wang Q. Wang. Study on Hydraulic and Thermal Performance of Printed Circuit Heat Transfer Surface with Distributed Airfoil Fins. *Appl. Therm. Eng.* 2017. **114**:1309–18.
23. Shi Z., Dong T. Entropy Generation and Optimization of Laminar Convective Heat Transfer and Fluid Flow in a Microchannel with Staggered Arrays of Pin Fin Structure with Tip Clearance. *Energy Convers. Manag.* 2015. **94**:493–504.
24. Chen F., Zhang L., Huai X., Li J., Zhang H., Liu Z. Comprehensive Performance Comparison of Airfoil Fin PCHEs with NACA 00XX Series Airfoil. *Nucl. Eng. Des.* 2017. **315**:42–50.
25. Yunus Cengel A Heat Transference a Practical Approach. MacGraw-Hill,. 2008. **4**(9):874.
26. Parker.com *Heatric Printed Circuit Heat Exchanger* [Accessed: 18 February 2025]. Available from: <https://www.parker.com/gb/en/divisions/heatric-c-division/resources/heat-exchangers.html>.

## APPENDIX

Nomenclature of formulae	Symbol	Unit
Overall Heat transfer coefficient in channel A	$U_A$	W/(m <sup>2</sup> .K)
Heat flow rate in a channel	$dQ$	Watt (W)
Temperature boundary channel	$T_{wall}$	Kelvin (K)
Channel outer temperature	$T_{out}$	Kelvin (K)
Channel inlet temperature	$T_{in}$	Kelvin (K)
Nusselt number	$N_u$	
hydrodynamic diameter.	$D_h$	mm
thermal conductivity	$k$	W/(m.K)
cross-sectional area	$A$	mm <sup>2</sup>
wetted perimeter of the fluid flow	$P$	mm
Pressure drop	$\Delta P$	Pa
Reynolds number	$Re_D$	
fluid density	$\rho$	kg/m <sup>3</sup>
velocity of the fluid	$v$	m/s
length of the channel	$L$	Mm
Viscosity of the fluid	$\mu$	Kg/(m.s)
Fin area temperature	$T_b$	°C
area of the fin from its base (the plate)	$A_b$	mm <sup>2</sup>
Height of the fin	$H_b$	Mm
ambient temperature of the environment	$T_\infty$	°C
convection coefficient between the fin and the ambient environment	$h$	W/(m <sup>2</sup> .K)
cross-sectional area of the fin at location $x$	$A_c(x)$	mm <sup>2</sup>
surface area around the perimeter of the differential element	$dA_s$	mm
heat flow rate from the surface area around the perimeter of the differential element, by convection	$dq_{conv}$	W/(m <sup>2</sup> .K)
heat flow rate conduction into the element at location $x$	$q(x)$	W/(m <sup>2</sup> .K)
heat flow rate initial condition	$q_f(0)$	W/(m <sup>2</sup> .K)
heat flow rate initial condition	$q_b(0)$	W/(m <sup>2</sup> .K)

## APPENDIX

Nomenclature of formulae	Symbol	Unit
Overall Heat transfer coefficient in channel A	$U_A$	W/(m <sup>2</sup> .K)
Heat flow rate in a channel	$dQ$	Watt (W)
Temperature boundary channel	$T_{wall}$	Kelvin (K)
Channel outer temperature	$T_{out}$	Kelvin (K)
Channel inlet temperature	$T_{in}$	Kelvin (K)
Nusselt number	$N_u$	
hydrodynamic diameter.	$D_h$	mm
thermal conductivity	$k$	W/(m.K)
cross-sectional area	$A$	mm <sup>2</sup>
wetted perimeter of the fluid flow	$P$	mm
Pressure drop	$\Delta P$	Pa
Reynolds number	$Re_D$	
fluid density	$\rho$	kg/m <sup>3</sup>
velocity of the fluid	$v$	m/s
length of the channel	$L$	Mm
Viscosity of the fluid	$\mu$	Kg/(m.s)
Fin area temperature	$T_b$	°C
area of the fin from its base (the plate)	$A_b$	mm <sup>2</sup>
Height of the fin	$H_b$	Mm
ambient temperature of the environment	$T_\infty$	°C
convection coefficient between the fin and the ambient environment	$h$	W/(m <sup>2</sup> .K)
cross-sectional area of the fin at location $x$	$A_c(x)$	mm <sup>2</sup>
surface area around the perimeter of the differential element	$dA_s$	mm
heat flow rate from the surface area around the perimeter of the differential element, by convection	$dq_{conv}$	W/(m <sup>2</sup> .K)
heat flow rate conduction into the element at location $x$	$q(x)$	W/(m <sup>2</sup> .K)
heat flow rate initial condition	$q_f(0)$	W/(m <sup>2</sup> .K)
heat flow rate initial condition	$q_b(0)$	W/(m <sup>2</sup> .K)